



Observation of photon polarization in the $b \rightarrow s\gamma$ transition

The LHCb collaboration[†]

Abstract

This Letter presents a study of the flavor-changing neutral current radiative $B^\pm \rightarrow K^\pm \pi^\mp \pi^\pm \gamma$ decays performed using data collected in proton-proton collisions with the LHCb detector at 7 and 8 TeV center-of-mass energies. In this sample, corresponding to an integrated luminosity of 3 fb^{-1} , nearly 14 000 signal events are reconstructed and selected, containing all possible intermediate resonances with a $K^\pm \pi^\mp \pi^\pm$ final state in the $[1.1, 1.9] \text{ GeV}/c^2$ mass range. The distribution of the angle of the photon direction with respect to the plane defined by the final-state hadrons in their rest frame is studied in intervals of $K^\pm \pi^\mp \pi^\pm$ mass and the asymmetry between the number of signal events found on each side of the plane is obtained. The first direct observation of the photon polarization in the $b \rightarrow s\gamma$ transition is reported with a significance of 5.2σ .

Published in Phys. Rev. Lett. 112, 161801 (2014)

© CERN on behalf of the LHCb collaboration, license CC-BY-3.0.

[†]Authors are listed on the following pages.

LHCb collaboration

R. Aaij⁴¹, B. Adeva³⁷, M. Adinolfi⁴⁶, A. Affolder⁵², Z. Ajaltouni⁵, J. Albrecht⁹, F. Alessio³⁸, M. Alexander⁵¹, S. Ali⁴¹, G. Alkhazov³⁰, P. Alvarez Cartelle³⁷, A.A. Alves Jr²⁵, S. Amato², S. Amerio²², Y. Amhis⁷, L. Anderlini^{17,g}, J. Anderson⁴⁰, R. Andreassen⁵⁷, M. Andreotti^{16,f}, J.E. Andrews⁵⁸, R.B. Appleby⁵⁴, O. Aquines Gutierrez¹⁰, F. Archilli³⁸, A. Artamonov³⁵, M. Artuso⁵⁹, E. Aslanides⁶, G. Auriemma^{25,m}, M. Baalouch⁵, S. Bachmann¹¹, J.J. Back⁴⁸, A. Badalov³⁶, V. Balagura³¹, W. Baldini¹⁶, R.J. Barlow⁵⁴, C. Barschel³⁹, S. Barsuk⁷, W. Barter⁴⁷, V. Batozskaya²⁸, Th. Bauer⁴¹, A. Bay³⁹, J. Beddow⁵¹, F. Bedeschi²³, I. Bediaga¹, S. Belogurov³¹, K. Belous³⁵, I. Belyaev³¹, E. Ben-Haim⁸, G. Bencivenni¹⁸, S. Benson⁵⁰, J. Benton⁴⁶, A. Berezhnoy³², R. Bernet⁴⁰, M.-O. Bettler⁴⁷, M. van Beuzekom⁴¹, A. Bien¹¹, S. Bifani⁴⁵, T. Bird⁵⁴, A. Bizzeti^{17,i}, P.M. Bjørnstad⁵⁴, T. Blake⁴⁸, F. Blanc³⁹, J. Blouw¹⁰, S. Blusk⁵⁹, V. Bocci²⁵, A. Bondar³⁴, N. Bondar³⁰, W. Bonivento^{15,38}, S. Borghi⁵⁴, A. Borgia⁵⁹, M. Borsato⁷, T.J.V. Bowcock⁵², E. Bowen⁴⁰, C. Bozzi¹⁶, T. Brambach⁹, J. van den Brand⁴², J. Bressieux³⁹, D. Brett⁵⁴, M. Britsch¹⁰, T. Britton⁵⁹, N.H. Brook⁴⁶, H. Brown⁵², A. Bursche⁴⁰, G. Busetto^{22,q}, J. Buytaert³⁸, S. Cadeddu¹⁵, R. Calabrese^{16,f}, O. Callot⁷, M. Calvi^{20,k}, M. Calvo Gomez^{36,o}, A. Camboni³⁶, P. Campana^{18,38}, D. Campora Perez³⁸, F. Caponio²¹, A. Carbone^{14,d}, G. Carboni^{24,l}, R. Cardinale^{19,j}, A. Cardini¹⁵, H. Carranza-Mejia⁵⁰, L. Carson⁵⁰, K. Carvalho Akiba², G. Casse⁵², L. Cassina²⁰, L. Castillo Garcia³⁸, M. Cattaneo³⁸, Ch. Cauet⁹, R. Cenci⁵⁸, M. Charles⁸, Ph. Charpentier³⁸, S.-F. Cheung⁵⁵, N. Chiapolini⁴⁰, M. Chrzaszcz^{40,26}, K. Ciba³⁸, X. Cid Vidal³⁸, G. Ciezarek⁵³, P.E.L. Clarke⁵⁰, M. Clemencic³⁸, H.V. Cliff⁴⁷, J. Closier³⁸, C. Coca²⁹, V. Coco³⁸, J. Cogan⁶, E. Cogneras⁵, P. Collins³⁸, A. Comerma-Montells³⁶, A. Contu^{15,38}, A. Cook⁴⁶, M. Coombes⁴⁶, S. Coquereau⁸, G. Corti³⁸, I. Counts⁵⁶, B. Couturier³⁸, G.A. Cowan⁵⁰, D.C. Craik⁴⁸, M. Cruz Torres⁶⁰, S. Cunliffe⁵³, R. Currie⁵⁰, C. D'Ambrosio³⁸, J. Dalseno⁴⁶, P. David⁸, P.N.Y. David⁴¹, A. Davis⁵⁷, I. De Bonis⁴, K. De Bruyn⁴¹, S. De Capua⁵⁴, M. De Cian¹¹, J.M. De Miranda¹, L. De Paula², W. De Silva⁵⁷, P. De Simone¹⁸, D. Decamp⁴, M. Deckenhoff⁹, L. Del Buono⁸, N. Déleage⁴, D. Derkach⁵⁵, O. Deschamps⁵, F. Dettori⁴², A. Di Canto¹¹, H. Dijkstra³⁸, S. Donleavy⁵², F. Dordei¹¹, M. Dorigo³⁹, P. Dorosz^{26,n}, A. Dosil Suárez³⁷, D. Dossett⁴⁸, A. Dovbnya⁴³, F. Dupertuis³⁹, P. Durante³⁸, R. Dzhelyadin³⁵, A. Dziurda²⁶, A. Dzyuba³⁰, S. Easo⁴⁹, U. Egede⁵³, V. Egorychev³¹, S. Eidelman³⁴, S. Eisenhardt⁵⁰, U. Eitschberger⁹, R. Ekelhof⁹, L. Eklund^{51,38}, I. El Rifai⁵, Ch. Elsasser⁴⁰, S. Esen¹¹, A. Falabella^{16,f}, C. Färber¹¹, C. Farinelli⁴¹, S. Farry⁵², D. Ferguson⁵⁰, V. Fernandez Albor³⁷, F. Ferreira Rodrigues¹, M. Ferro-Luzzi³⁸, S. Filippov³³, M. Fiore^{16,f}, M. Fiorini^{16,f}, C. Fitzpatrick³⁸, M. Fontana¹⁰, F. Fontanelli^{19,j}, R. Forty³⁸, O. Francisco², M. Frank³⁸, C. Frei³⁸, M. Frosini^{17,38,g}, J. Fu²¹, E. Furfaro^{24,l}, A. Gallas Torreira³⁷, D. Galli^{14,d}, S. Gambetta^{19,j}, M. Gandelman², P. Gandini⁵⁹, Y. Gao³, J. Garofoli⁵⁹, J. Garra Tico⁴⁷, L. Garrido³⁶, C. Gaspar³⁸, R. Gauld⁵⁵, L. Gavardi⁹, E. Gersabeck¹¹, M. Gersabeck⁵⁴, T. Gershon⁴⁸, Ph. Ghez⁴, A. Gianelle²², S. Giani³⁹, V. Gibson⁴⁷, L. Giubega²⁹, V.V. Gligorov³⁸, C. Göbel⁶⁰, D. Golubkov³¹, A. Golutvin^{53,31,38}, A. Gomes^{1,a}, H. Gordon³⁸, M. Grabalosa Gándara⁵, R. Graciani Diaz³⁶, L.A. Granado Cardoso³⁸, E. Graugés³⁶, G. Graziani¹⁷, A. Greco²⁹, E. Greening⁵⁵, S. Gregson⁴⁷, P. Griffith⁴⁵, L. Grillo¹¹, O. Grünberg⁶¹, B. Gui⁵⁹, E. Gushchin³³, Yu. Guz^{35,38}, T. Gys³⁸, C. Hadjivasiliou⁵⁹, G. Haefeli³⁹, C. Haen³⁸, T.W. Hafkenscheid⁶⁴, S.C. Haines⁴⁷, S. Hall⁵³, B. Hamilton⁵⁸, T. Hampson⁴⁶, S. Hansmann-Menzemer¹¹, N. Harnew⁵⁵, S.T. Harnew⁴⁶, J. Harrison⁵⁴, T. Hartmann⁶¹, J. He³⁸, T. Head³⁸, V. Heijne⁴¹, K. Hennessy⁵², P. Henrard⁵, L. Henry⁸, J.A. Hernando Morata³⁷, E. van Herwijnen³⁸, M. Heß⁶¹, A. Hicheur¹, D. Hill⁵⁵,

M. Hoballah⁵, C. Hombach⁵⁴, W. Hulsbergen⁴¹, P. Hunt⁵⁵, N. Hussain⁵⁵, D. Hutchcroft⁵²,
D. Hynds⁵¹, M. Idzik²⁷, P. Ilten⁵⁶, R. Jacobsson³⁸, A. Jaeger¹¹, E. Jans⁴¹, P. Jatou³⁹,
A. Jawahery⁵⁸, F. Jing³, M. John⁵⁵, D. Johnson⁵⁵, C.R. Jones⁴⁷, C. Joram³⁸, B. Jost³⁸,
N. Jurik⁵⁹, M. Kaballo⁹, S. Kandybei⁴³, W. Kanso⁶, M. Karacson³⁸, T.M. Karbach³⁸,
M. Kelsey⁵⁹, I.R. Kenyon⁴⁵, T. Ketel⁴², B. Khanji²⁰, C. Khurewathanakul³⁹, S. Klaver⁵⁴,
O. Kochebina⁷, I. Komarov³⁹, R.F. Koopman⁴², P. Koppenburg⁴¹, M. Korolev³²,
A. Kozlinskiy⁴¹, L. Kravchuk³³, K. Kreplin¹¹, M. Kreps⁴⁸, G. Krocker¹¹, P. Krokovny³⁴,
F. Kruse⁹, M. Kucharczyk^{20,26,38,k}, V. Kudryavtsev³⁴, K. Kurek²⁸, T. Kvaratskheliya^{31,38},
V.N. La Thi³⁹, D. Lacarrere³⁸, G. Lafferty⁵⁴, A. Lai¹⁵, D. Lambert⁵⁰, R.W. Lambert⁴²,
E. Lanciotti³⁸, G. Lanfranchi¹⁸, C. Langenbruch³⁸, B. Langhans³⁸, T. Latham⁴⁸, C. Lazzeroni⁴⁵,
R. Le Gac⁶, J. van Leerdam⁴¹, J.-P. Lees⁴, R. Lefèvre⁵, A. Leflat³², J. Lefrançois⁷, S. Leo²³,
O. Leroy⁶, T. Lesiak²⁶, B. Leverington¹¹, Y. Li³, M. Liles⁵², R. Lindner³⁸, C. Linn³⁸,
F. Lionetto⁴⁰, B. Liu¹⁵, G. Liu³⁸, S. Lohn³⁸, I. Longstaff⁵¹, J.H. Lopes², N. Lopez-March³⁹,
P. Lowdon⁴⁰, H. Lu³, D. Lucchesi^{22,q}, H. Luo⁵⁰, E. Luppi^{16,f}, O. Lupton⁵⁵, F. Machefert⁷,
I.V. Machikhiliyan³¹, F. Maciuc²⁹, O. Maev^{30,38}, S. Malde⁵⁵, G. Manca^{15,e}, G. Mancinelli⁶,
M. Manzali^{16,f}, J. Maratas⁵, U. Marconi¹⁴, C. Marin Benito³⁶, P. Marino^{23,s}, R. Märki³⁹,
J. Marks¹¹, G. Martellotti²⁵, A. Martens⁸, A. Martín Sánchez⁷, M. Martinelli⁴¹,
D. Martinez Santos⁴², F. Martinez Vidal⁶³, D. Martins Tostes², A. Massafferri¹, R. Matev³⁸,
Z. Mathe³⁸, C. Matteuzzi²⁰, A. Mazurov^{16,38,f}, M. McCann⁵³, J. McCarthy⁴⁵, A. McNab⁵⁴,
R. McNulty¹², B. McSkelly⁵², B. Meadows^{57,55}, F. Meier⁹, M. Meissner¹¹, M. Merk⁴¹,
D.A. Milanese⁸, M.-N. Minard⁴, J. Molina Rodriguez⁶⁰, S. Monteil⁵, D. Moran⁵⁴, M. Morandin²²,
P. Morawski²⁶, A. Mordà⁶, M.J. Morello^{23,s}, R. Mountain⁵⁹, F. Muheim⁵⁰, K. Müller⁴⁰,
R. Muresan²⁹, B. Muryn²⁷, B. Muster³⁹, P. Naik⁴⁶, T. Nakada³⁹, R. Nandakumar⁴⁹, I. Nasteva¹,
M. Needham⁵⁰, N. Neri²¹, S. Neubert³⁸, N. Neufeld³⁸, A.D. Nguyen³⁹, T.D. Nguyen³⁹,
C. Nguyen-Mau^{39,p}, M. Nicol⁷, V. Niess⁵, R. Niet⁹, N. Nikitin³², T. Nikodem¹¹, A. Novoselov³⁵,
A. Oblakowska-Mucha²⁷, V. Obraztsov³⁵, S. Oggero⁴¹, S. Ogilvy⁵¹, O. Okhrimenko⁴⁴,
R. Oldeman^{15,e}, G. Onderwater⁶⁴, M. Orlandea²⁹, J.M. Otalora Goicochea², P. Owen⁵³,
A. Oyanguren³⁶, B.K. Pal⁵⁹, A. Palano^{13,c}, F. Palombo^{21,t}, M. Palutan¹⁸, J. Panman³⁸,
A. Papanestis^{49,38}, M. Pappagallo⁵¹, L. Pappalardo¹⁶, C. Parkes⁵⁴, C.J. Parkinson⁹,
G. Passaleva¹⁷, G.D. Patel⁵², M. Patel⁵³, C. Patrignani^{19,j}, C. Pavel-Nicorescu²⁹,
A. Pazos Alvarez³⁷, A. Pearce⁵⁴, A. Pellegrino⁴¹, M. Pepe Altarelli³⁸, S. Perazzini^{14,d},
E. Perez Trigo³⁷, P. Perret⁵, M. Perrin-Terrin⁶, L. Pescatore⁴⁵, E. Pesen⁶⁵, G. Pessina²⁰,
K. Petridis⁵³, A. Petrolini^{19,j}, E. Picatoste Olloqui³⁶, B. Pietrzyk⁴, T. Pilař⁴⁸, D. Pinci²⁵,
A. Pistone¹⁹, S. Playfer⁵⁰, M. Plo Casasus³⁷, F. Polci⁸, A. Poluektov^{48,34}, E. Polycarpo²,
A. Popov³⁵, D. Popov¹⁰, B. Popovici²⁹, C. Potterat³⁶, A. Powell⁵⁵, J. Prisciandaro³⁹,
A. Pritchard⁵², C. Prouve⁴⁶, V. Pugatch⁴⁴, A. Puig Navarro³⁹, G. Punzi^{23,r}, W. Qian⁴,
B. Rachwal²⁶, J.H. Rademacker⁴⁶, B. Rakotomiamanana³⁹, M. Rama¹⁸, M.S. Rangel²,
I. Raniuk⁴³, N. Rauschmayr³⁸, G. Raven⁴², S. Reichert⁵⁴, M.M. Reid⁴⁸, A.C. dos Reis¹,
S. Ricciardi⁴⁹, A. Richards⁵³, K. Rinnert⁵², V. Rives Molina³⁶, D.A. Roa Romero⁵, P. Robbe⁷,
D.A. Roberts⁵⁸, A.B. Rodrigues¹, E. Rodrigues⁵⁴, P. Rodriguez Perez³⁷, S. Roiser³⁸,
V. Romanovsky³⁵, A. Romero Vidal³⁷, M. Rotondo²², J. Rouvinet³⁹, T. Ruf³⁸, F. Ruffini²³,
H. Ruiz³⁶, P. Ruiz Valls³⁶, G. Sabatino^{25,l}, J.J. Saborido Silva³⁷, N. Sagidova³⁰, P. Sail⁵¹,
B. Saitta^{15,e}, V. Salustino Guimaraes², B. Sanmartin Sedes³⁷, R. Santacesaria²⁵,
C. Santamarina Rios³⁷, E. Santovetti^{24,l}, M. Sapunov⁶, A. Sarti¹⁸, C. Satriano^{25,m}, A. Satta²⁴,
M. Savrie^{16,f}, D. Savrina^{31,32}, M. Schiller⁴², H. Schindler³⁸, M. Schlupp⁹, M. Schmelling¹⁰,
B. Schmidt³⁸, O. Schneider³⁹, A. Schopper³⁸, M.-H. Schune⁷, R. Schwemmer³⁸, B. Sciascia¹⁸,

A. Sciubba²⁵, M. Seco³⁷, A. Semennikov³¹, K. Senderowska²⁷, I. Sepp⁵³, N. Serra⁴⁰, J. Serrano⁶, P. Seyfert¹¹, M. Shapkin³⁵, I. Shapoval^{16,43,f}, Y. Shcheglov³⁰, T. Shears⁵², L. Shekhtman³⁴, O. Shevchenko⁴³, V. Shevchenko⁶², A. Shires⁹, R. Silva Coutinho⁴⁸, G. Simi²², M. Sirendi⁴⁷, N. Skidmore⁴⁶, T. Skwarnicki⁵⁹, N.A. Smith⁵², E. Smith^{55,49}, E. Smith⁵³, J. Smith⁴⁷, M. Smith⁵⁴, H. Snoek⁴¹, M.D. Sokoloff⁵⁷, F.J.P. Soler⁵¹, F. Soomro³⁹, D. Souza⁴⁶, B. Souza De Paula², B. Spaan⁹, A. Sparkes⁵⁰, F. Spinella²³, P. Spradlin⁵¹, F. Stagni³⁸, S. Stahl¹¹, O. Steinkamp⁴⁰, S. Stevenson⁵⁵, S. Stoica²⁹, S. Stone⁵⁹, B. Storaci⁴⁰, S. Stracka^{23,38}, M. Straticiu²⁹, U. Straumann⁴⁰, R. Stroili²², V.K. Subbiah³⁸, L. Sun⁵⁷, W. Sutcliffe⁵³, S. Swientek⁹, V. Syropoulos⁴², M. Szczekowski²⁸, P. Szczypka^{39,38}, D. Szilard², T. Szumlak²⁷, S. T’Jampens⁴, M. Teklishyn⁷, G. Tellarini^{16,f}, E. Teodorescu²⁹, F. Teubert³⁸, C. Thomas⁵⁵, E. Thomas³⁸, J. van Tilburg¹¹, V. Tisserand⁴, M. Tobin³⁹, S. Tolk⁴², L. Tomassetti^{16,f}, D. Tonelli³⁸, S. Topp-Joergensen⁵⁵, N. Torr⁵⁵, E. Tournefier^{4,53}, S. Tourneur³⁹, M.T. Tran³⁹, M. Tresch⁴⁰, A. Tsaregorodtsev⁶, P. Tsopelas⁴¹, N. Tuning⁴¹, M. Ubeda Garcia³⁸, A. Ukleja²⁸, A. Ustyuzhanin⁶², U. Uwer¹¹, V. Vagnoni¹⁴, G. Valenti¹⁴, A. Vallier⁷, R. Vazquez Gomez¹⁸, P. Vazquez Regueiro³⁷, C. Vázquez Sierra³⁷, S. Vecchi¹⁶, J.J. Velthuis⁴⁶, M. Veltri^{17,h}, G. Veneziano³⁹, M. Vesterinen¹¹, B. Viaud⁷, D. Vieira², X. Vilasis-Cardona^{36,o}, A. Vollhardt⁴⁰, D. Volyanskyy¹⁰, D. Voong⁴⁶, A. Vorobyev³⁰, V. Vorobyev³⁴, C. Voß⁶¹, H. Voss¹⁰, J.A. de Vries⁴¹, R. Waldi⁶¹, C. Wallace⁴⁸, R. Wallace¹², S. Wandernoth¹¹, J. Wang⁵⁹, D.R. Ward⁴⁷, N.K. Watson⁴⁵, A.D. Webber⁵⁴, D. Websdale⁵³, M. Whitehead⁴⁸, J. Wicht³⁸, J. Wiechczynski²⁶, D. Wiedner¹¹, G. Wilkinson⁵⁵, M.P. Williams^{48,49}, M. Williams⁵⁶, F.F. Wilson⁴⁹, J. Wimberley⁵⁸, J. Wishahi⁹, W. Wislicki²⁸, M. Witek²⁶, G. Wormser⁷, S.A. Wotton⁴⁷, S. Wright⁴⁷, S. Wu³, K. Wyllie³⁸, Y. Xie^{50,38}, Z. Xing⁵⁹, Z. Yang³, X. Yuan³, O. Yushchenko³⁵, M. Zangoli¹⁴, M. Zavertyaev^{10,b}, F. Zhang³, L. Zhang⁵⁹, W.C. Zhang¹², Y. Zhang³, A. Zhelezov¹¹, A. Zhokhov³¹, L. Zhong³, A. Zvyagin³⁸.

¹Centro Brasileiro de Pesquisas Físicas (CBPF), Rio de Janeiro, Brazil

²Universidade Federal do Rio de Janeiro (UFRJ), Rio de Janeiro, Brazil

³Center for High Energy Physics, Tsinghua University, Beijing, China

⁴LAPP, Université de Savoie, CNRS/IN2P3, Annecy-Le-Vieux, France

⁵Clermont Université, Université Blaise Pascal, CNRS/IN2P3, LPC, Clermont-Ferrand, France

⁶CPPM, Aix-Marseille Université, CNRS/IN2P3, Marseille, France

⁷LAL, Université Paris-Sud, CNRS/IN2P3, Orsay, France

⁸LPNHE, Université Pierre et Marie Curie, Université Paris Diderot, CNRS/IN2P3, Paris, France

⁹Fakultät Physik, Technische Universität Dortmund, Dortmund, Germany

¹⁰Max-Planck-Institut für Kernphysik (MPIK), Heidelberg, Germany

¹¹Physikalisches Institut, Ruprecht-Karls-Universität Heidelberg, Heidelberg, Germany

¹²School of Physics, University College Dublin, Dublin, Ireland

¹³Sezione INFN di Bari, Bari, Italy

¹⁴Sezione INFN di Bologna, Bologna, Italy

¹⁵Sezione INFN di Cagliari, Cagliari, Italy

¹⁶Sezione INFN di Ferrara, Ferrara, Italy

¹⁷Sezione INFN di Firenze, Firenze, Italy

¹⁸Laboratori Nazionali dell’INFN di Frascati, Frascati, Italy

¹⁹Sezione INFN di Genova, Genova, Italy

²⁰Sezione INFN di Milano Bicocca, Milano, Italy

²¹Sezione INFN di Milano, Milano, Italy

²²Sezione INFN di Padova, Padova, Italy

²³Sezione INFN di Pisa, Pisa, Italy

²⁴Sezione INFN di Roma Tor Vergata, Roma, Italy

- ²⁵ *Sezione INFN di Roma La Sapienza, Roma, Italy*
- ²⁶ *Henryk Niewodniczanski Institute of Nuclear Physics Polish Academy of Sciences, Kraków, Poland*
- ²⁷ *AGH - University of Science and Technology, Faculty of Physics and Applied Computer Science, Kraków, Poland*
- ²⁸ *National Center for Nuclear Research (NCBJ), Warsaw, Poland*
- ²⁹ *Horia Hulubei National Institute of Physics and Nuclear Engineering, Bucharest-Magurele, Romania*
- ³⁰ *Petersburg Nuclear Physics Institute (PNPI), Gatchina, Russia*
- ³¹ *Institute of Theoretical and Experimental Physics (ITEP), Moscow, Russia*
- ³² *Institute of Nuclear Physics, Moscow State University (SINP MSU), Moscow, Russia*
- ³³ *Institute for Nuclear Research of the Russian Academy of Sciences (INR RAN), Moscow, Russia*
- ³⁴ *Budker Institute of Nuclear Physics (SB RAS) and Novosibirsk State University, Novosibirsk, Russia*
- ³⁵ *Institute for High Energy Physics (IHEP), Protvino, Russia*
- ³⁶ *Universitat de Barcelona, Barcelona, Spain*
- ³⁷ *Universidad de Santiago de Compostela, Santiago de Compostela, Spain*
- ³⁸ *European Organization for Nuclear Research (CERN), Geneva, Switzerland*
- ³⁹ *Ecole Polytechnique Fédérale de Lausanne (EPFL), Lausanne, Switzerland*
- ⁴⁰ *Physik-Institut, Universität Zürich, Zürich, Switzerland*
- ⁴¹ *Nikhef National Institute for Subatomic Physics, Amsterdam, The Netherlands*
- ⁴² *Nikhef National Institute for Subatomic Physics and VU University Amsterdam, Amsterdam, The Netherlands*
- ⁴³ *NSC Kharkiv Institute of Physics and Technology (NSC KIPT), Kharkiv, Ukraine*
- ⁴⁴ *Institute for Nuclear Research of the National Academy of Sciences (KINR), Kyiv, Ukraine*
- ⁴⁵ *University of Birmingham, Birmingham, United Kingdom*
- ⁴⁶ *H.H. Wills Physics Laboratory, University of Bristol, Bristol, United Kingdom*
- ⁴⁷ *Cavendish Laboratory, University of Cambridge, Cambridge, United Kingdom*
- ⁴⁸ *Department of Physics, University of Warwick, Coventry, United Kingdom*
- ⁴⁹ *STFC Rutherford Appleton Laboratory, Didcot, United Kingdom*
- ⁵⁰ *School of Physics and Astronomy, University of Edinburgh, Edinburgh, United Kingdom*
- ⁵¹ *School of Physics and Astronomy, University of Glasgow, Glasgow, United Kingdom*
- ⁵² *Oliver Lodge Laboratory, University of Liverpool, Liverpool, United Kingdom*
- ⁵³ *Imperial College London, London, United Kingdom*
- ⁵⁴ *School of Physics and Astronomy, University of Manchester, Manchester, United Kingdom*
- ⁵⁵ *Department of Physics, University of Oxford, Oxford, United Kingdom*
- ⁵⁶ *Massachusetts Institute of Technology, Cambridge, MA, United States*
- ⁵⁷ *University of Cincinnati, Cincinnati, OH, United States*
- ⁵⁸ *University of Maryland, College Park, MD, United States*
- ⁵⁹ *Syracuse University, Syracuse, NY, United States*
- ⁶⁰ *Pontifícia Universidade Católica do Rio de Janeiro (PUC-Rio), Rio de Janeiro, Brazil, associated to ²*
- ⁶¹ *Institut für Physik, Universität Rostock, Rostock, Germany, associated to ¹¹*
- ⁶² *National Research Centre Kurchatov Institute, Moscow, Russia, associated to ³¹*
- ⁶³ *Instituto de Fisica Corpuscular (IFIC), Universitat de Valencia-CSIC, Valencia, Spain, associated to ³⁶*
- ⁶⁴ *KVI - University of Groningen, Groningen, The Netherlands, associated to ⁴¹*
- ⁶⁵ *Celal Bayar University, Manisa, Turkey, associated to ³⁸*

^a *Universidade Federal do Triângulo Mineiro (UFMT), Uberaba-MG, Brazil*

^b *P.N. Lebedev Physical Institute, Russian Academy of Science (LPI RAS), Moscow, Russia*

^c *Università di Bari, Bari, Italy*

^d *Università di Bologna, Bologna, Italy*

^e *Università di Cagliari, Cagliari, Italy*

^f *Università di Ferrara, Ferrara, Italy*

^g *Università di Firenze, Firenze, Italy*

^h *Università di Urbino, Urbino, Italy*

ⁱ *Università di Modena e Reggio Emilia, Modena, Italy*

^j *Università di Genova, Genova, Italy*

^k *Università di Milano Bicocca, Milano, Italy*

^l *Università di Roma Tor Vergata, Roma, Italy*

^m *Università della Basilicata, Potenza, Italy*

ⁿ *AGH - University of Science and Technology, Faculty of Computer Science, Electronics and Telecommunications, Kraków, Poland*

^o *LIFAELS, La Salle, Universitat Ramon Llull, Barcelona, Spain*

^p *Hanoi University of Science, Hanoi, Viet Nam*

^q *Università di Padova, Padova, Italy*

^r *Università di Pisa, Pisa, Italy*

^s *Scuola Normale Superiore, Pisa, Italy*

^t *Università degli Studi di Milano, Milano, Italy*

The Standard Model (SM) predicts that the photon emitted from the electroweak penguin loop in $b \rightarrow s\gamma$ transitions is predominantly left-handed, since the recoiling s quark that couples to a W boson is left-handed. This implies maximal parity violation up to small corrections of the order m_s/m_b . While the measured inclusive $b \rightarrow s\gamma$ rate [1] agrees with the SM calculations, no direct evidence exists for a nonzero photon polarization in this type of decays. Several extensions of the SM [2], compatible with all current measurements, predict that the photon acquires a significant right-handed component, in particular due to the exchange of a heavy fermion in the penguin loop [3].

This Letter presents a study of the radiative decay $B^+ \rightarrow K^+\pi^-\pi^+\gamma$, previously observed at the B factories with a measured branching fraction of $(27.6 \pm 2.2) \times 10^{-6}$ [1,4,5]. The inclusion of charge-conjugate processes is implied throughout. Information about the photon polarization is obtained from the angular distribution of the photon direction with respect to the normal to the plane defined by the momenta of the three final-state hadrons in their center-of-mass frame. The shape of this distribution, including the *up-down asymmetry* between the number of events with the photon on either side of the plane, is determined. This investigation is conceptually similar to the historical experiment that discovered parity violation by measuring the up-down asymmetry of the direction of a particle emitted in a weak decay with respect to an axial vector [6]. In $B^+ \rightarrow K^+\pi^-\pi^+\gamma$ decays, the up-down asymmetry is proportional to the photon polarization λ_γ [7,8] and therefore measuring a value different from zero corresponds to demonstrating that the photon is polarized. The currently limited knowledge of the structure of the $K^+\pi^-\pi^+$ mass spectrum, which includes interfering kaon resonances, prevents the translation of a measured asymmetry into an actual value for λ_γ .

The differential $B^+ \rightarrow K^+\pi^-\pi^+\gamma$ decay rate can be described in terms of θ , defined in the rest frame of the final state hadrons as the angle between the direction opposite to the photon momentum \vec{p}_γ and the normal $\vec{p}_{\pi,\text{slow}} \times \vec{p}_{\pi,\text{fast}}$ to the $K^+\pi^-\pi^+$ plane, where $\vec{p}_{\pi,\text{slow}}$ and $\vec{p}_{\pi,\text{fast}}$ correspond to the momenta of the lower and higher momentum pions, respectively. Following the notation and developments of Ref. [7], the differential decay rate of $B^+ \rightarrow K^+\pi^-\pi^+\gamma$ can be written as a fourth-order polynomial in $\cos\theta$

$$\frac{d\Gamma}{ds ds_{13} ds_{23} d\cos\theta} \propto \sum_{i=0,2,4} a_i(s, s_{13}, s_{23}) \cos^i\theta + \lambda_\gamma \sum_{j=1,3} a_j(s, s_{13}, s_{23}) \cos^j\theta, \quad (1)$$

where $s_{ij} = (p_i + p_j)^2$ and $s = (p_1 + p_2 + p_3)^2$, and p_1 , p_2 and p_3 are the four-momenta of the π^- , π^+ and K^+ mesons, respectively. The functions a_k depend on the resonances present in the $K^+\pi^-\pi^+$ mass range of interest and their interferences. The up-down asymmetry is defined as

$$\mathcal{A}_{\text{ud}} \equiv \frac{\int_0^1 d\cos\theta \frac{d\Gamma}{d\cos\theta} - \int_{-1}^0 d\cos\theta \frac{d\Gamma}{d\cos\theta}}{\int_{-1}^1 d\cos\theta \frac{d\Gamma}{d\cos\theta}}, \quad (2)$$

which is proportional to λ_γ .

The LHCb detector [9] is a single-arm forward spectrometer covering the pseudorapidity range $2 < \eta < 5$, designed for the study of particles containing b or c quarks. The detector includes a high-precision tracking system consisting of a silicon-strip vertex detector

surrounding the pp interaction region, a large-area silicon-strip detector located upstream of a dipole magnet with a bending power of about 4 Tm, and three stations of silicon-strip detectors and straw drift tubes placed downstream. The combined tracking system provides a momentum measurement with relative uncertainty that varies from 0.4% at 5 GeV/ c to 0.6% at 100 GeV/ c , and impact parameter resolution of 20 μm for tracks with a few GeV/ c of transverse momentum (p_{T}). Different types of charged hadrons are distinguished by information from two ring-imaging Cherenkov detectors. Photon, electron and hadron candidates are identified by a calorimeter system consisting of scintillating-pad and preshower detectors, an electromagnetic calorimeter and a hadronic calorimeter. The trigger consists of a hardware stage, based on information from the calorimeter and muon systems, followed by a software stage, which applies a full event reconstruction.

Samples of simulated events are used to understand signal and backgrounds. In the simulation, pp collisions are generated using PYTHIA [10] with a specific LHCb configuration [11]. Decays of hadronic particles are described by EVTGEN [12], in which final state radiation is generated using PHOTOS [13]. The interaction of the generated particles with the detector and its response are implemented using the GEANT4 toolkit [14] as described in Ref. [15].

This analysis is based on the LHCb data sample collected from pp collisions at 7 and 8 TeV center-of-mass energies in 2011 and 2012, respectively, corresponding to 3 fb^{-1} of integrated luminosity. The $B^+ \rightarrow K^+ \pi^- \pi^+ \gamma$ candidates are built from a photon candidate and a hadronic system reconstructed from a kaon and two oppositely charged pions satisfying particle identification requirements. Each of the hadrons is required to have a minimum p_{T} of 0.5 GeV/ c and at least one of them needs to have a p_{T} larger than 1.2 GeV/ c . The isolation of the $K^+ \pi^- \pi^+$ vertex from other tracks in the event is ensured by requiring that the χ^2 of the three-track vertex fit and the χ^2 of all possible vertices that can be obtained by adding an extra track differ by more than 2. The $K^+ \pi^- \pi^+$ mass is required to be in the [1.1, 1.9] GeV/ c^2 range. High transverse energy (> 3.0 GeV) photon candidates are constructed from energy depositions in the electromagnetic calorimeter. The absence of tracks pointing to the calorimeter is used to distinguish neutral from charged electromagnetic particles. A multivariate algorithm based on the energy cluster shape parameters is used to reject approximately 65% of the $\pi^0 \rightarrow \gamma\gamma$ background in which the two photons are reconstructed as a single cluster, while keeping about 95% of the signal photons. The B^+ candidate mass is required to be in the [4.3, 6.9] GeV/ c^2 range. Backgrounds that are expected to peak in this mass range are suppressed by removing all candidates consistent with a $\bar{D}^0 \rightarrow K^+ \pi^- \pi^0$ or $\rho^+ \rightarrow \pi^+ \pi^0$ decay when the photon candidate is assumed to be a π^0 .

A boosted decision tree [16, 17] is used to further improve the separation between signal and background. Its training is based on the following variables: the impact parameter χ^2 of the B^+ meson and of each of the final state hadrons, defined as the difference between the χ^2 of a primary vertex (PV) reconstructed with and without the considered particle; the cosine of the angle between the reconstructed B^+ momentum and the vector pointing from the PV to the B^+ decay vertex; the flight distance of the B^+ meson; and the $K^+ \pi^- \pi^+$ vertex χ^2 .

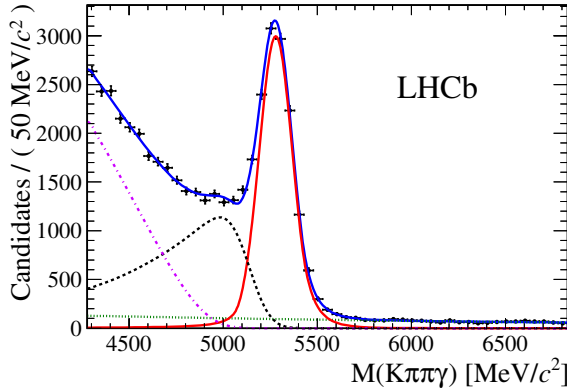


Figure 1: Mass distribution of the selected $B^+ \rightarrow K^+ \pi^- \pi^+ \gamma$ candidates. The blue solid curve shows the fit results as the sum of the following components: signal (red solid), combinatorial background (green dotted), missing pion background (black dashed) and other partially reconstructed backgrounds (purple dash-dotted).

The mass distribution of the selected $B^+ \rightarrow K^+ \pi^- \pi^+ \gamma$ signal is modeled with a double-tailed Crystal Ball [18] probability density function (PDF), with power-law tails above and below the B mass. The four tail parameters are fixed from simulation; the width of the signal peak is fit separately for 2011 and 2012 data to account for differences in calorimeter calibration. Combinatorial and partially reconstructed backgrounds are considered in the fit, the former modeled with an exponential PDF, the latter described using an ARGUS PDF [19] convolved with a Gaussian function with the same width as the signal to account for the photon energy resolution. The contribution to the partially reconstructed background from events with only one missing pion is considered separately.

The fit of the mass distribution of the selected $B^+ \rightarrow K^+ \pi^- \pi^+ \gamma$ candidates (Fig. 1) returns a total signal yield of 13876 ± 153 events, the largest sample recorded for this channel to date. Figure 2 shows the background-subtracted $K^+ \pi^- \pi^+$ mass spectrum determined using the technique of Ref. [20], after constraining the B mass to its nominal value. No peak other than that of the $K_1(1270)^+$ resonance can be clearly identified. Many kaon resonances, with various masses, spins and angular momenta, are expected to contribute and interfere in the considered mass range [1].

The contributions from single resonances cannot be isolated because of the complicated structure of the $K^+ \pi^- \pi^+$ mass spectrum. The up-down asymmetry is thus studied inclusively in four intervals of $K^+ \pi^- \pi^+$ mass. The $[1.4, 1.6]$ GeV/c^2 interval, studied in Ref. [7], includes the $K_1(1400)^+$, $K_2^*(1430)^+$ and $K^*(1410)^+$ resonances with small contributions from the upper tail of the $K_1(1270)^+$. At the time of the writing of Ref. [7], the $K_1(1400)^+$ was believed to be the dominant 1^+ resonance, so the $K_1(1270)^+$ was not considered. However, subsequent experimental results [21] demonstrated that the $K_1(1270)^+$ is more prominent than the $K_1(1400)^+$, hence the $[1.1, 1.3]$ GeV/c^2 interval is also studied here. The $[1.3, 1.4]$ GeV/c^2 mass interval, which contains the overlap region between the two K_1 resonances, and the $[1.6, 1.9]$ GeV/c^2 high mass interval, which includes

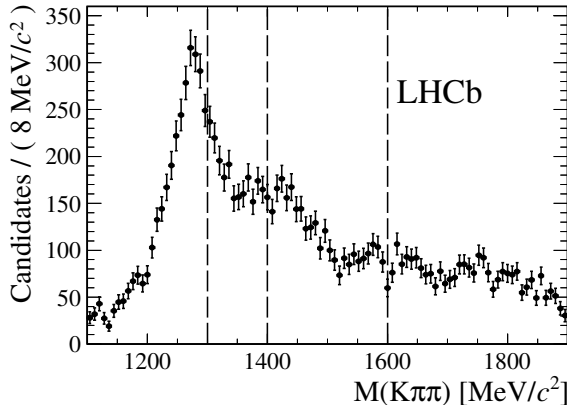


Figure 2: Background-subtracted $K^+\pi^-\pi^+$ mass distribution of the $B^+ \rightarrow K^+\pi^-\pi^+\gamma$ signal. The four intervals of interest, separated by dashed lines, are shown.

spin-2 and spin-3 resonances, are also considered.

In each of the four $K^+\pi^-\pi^+$ mass intervals, a simultaneous fit to the B -candidate mass spectra in bins of the photon angle is performed in order to determine the background-subtracted angular distribution; the previously described PDF is used to model the mass spectrum in each bin, with all of the fit parameters being shared except for the yields. Since the sign of the photon polarization depends on the sign of the electric charge of the B candidate, the angular variable $\cos \hat{\theta} \equiv \text{charge}(B) \cos \theta$ is used. The resulting background-subtracted $\cos \hat{\theta}$ distribution, corrected for the selection acceptance and normalized to the inverse of the bin width, is fit with a fourth-order polynomial function normalized to unit area,

$$f(\cos \hat{\theta}; c_0=0.5, c_1, c_2, c_3, c_4) = \sum_{i=0}^4 c_i L_i(\cos \hat{\theta}), \quad (3)$$

where $L_i(x)$ is the Legendre polynomial of order i and c_i is the corresponding coefficient. Using Eqs. 1 and 3 the up-down asymmetry defined in Eq. 2 can be expressed as

$$\mathcal{A}_{\text{ud}} = c_1 - \frac{c_3}{4}. \quad (4)$$

As a cross-check, the up-down asymmetry in each mass interval is also determined with a counting method, rather than an angular fit, as well as considering separately the B^+ and B^- candidates. All these checks yield compatible results.

The results obtained from a χ^2 fit of the normalized binned angular distribution, performed taking into account the full covariance matrix of the bin contents and all of the systematic uncertainties, are summarized in Table 1. These systematic uncertainties account for the effect of choosing a different fit model, the impact of the limited size of the simulated samples on the fixed parameters, and the possibility of some events migrating from a bin to its neighbor because of the detector resolution, which gives the dominant contribution. The systematic uncertainty associated with the fit model is determined by

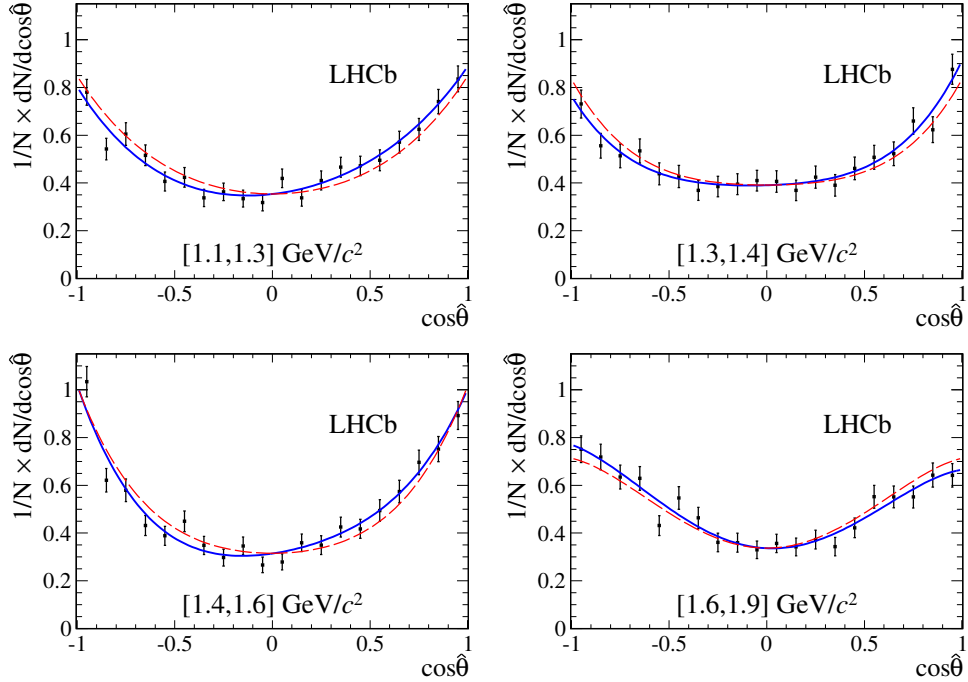


Figure 3: Distributions of $\cos \hat{\theta}$ for $B^+ \rightarrow K^+ \pi^- \pi^+ \gamma$ signal in four intervals of $K^+ \pi^- \pi^+$ mass. The solid blue (dashed red) curves are the result of fits allowing all (only even) Legendre components up to the fourth power.

performing the mass fit using several alternative PDFs, while the other two are estimated with simulated pseudoexperiments. Such uncertainties, despite being of the same size as the statistical uncertainty, do not substantially affect the fit results since they are strongly correlated across all angular bins.

The fitted distributions in the four $K^+ \pi^- \pi^+$ mass intervals of interest are shown in Fig. 3. In order to illustrate the effect of the up-down asymmetry, the results of another fit imposing $c_1 = c_3 = 0$, hence forbidding the terms that carry the λ_γ dependence, are overlaid for comparison.

The combined significance of the observed up-down asymmetries is determined from a χ^2 test where the null hypothesis is defined as $\lambda_\gamma = 0$, implying that the up-down asymmetry is expected to be zero in each mass interval. The corresponding χ^2 distribution has four degrees of freedom, and the observed value corresponds to a p-value of 1.7×10^{-7} . This translates into a 5.2σ significance for nonzero up-down asymmetry. Up-down asymmetries can be computed also for an alternative definition of the photon angle, obtained using the normal $\vec{p}_{\pi^-} \times \vec{p}_{\pi^+}$ instead of $\vec{p}_{\pi, \text{slow}} \times \vec{p}_{\pi, \text{fast}}$. The obtained values, along with the relative fit coefficients, are listed in Table 2.

To summarize, a study of the inclusive flavor-changing neutral current radiative $B^+ \rightarrow K^+ \pi^- \pi^+ \gamma$ decay, with the $K^+ \pi^- \pi^+$ mass in the $[1.1, 1.9]$ GeV/c^2 range, is performed on a data sample corresponding to an integrated luminosity of 3 fb^{-1} collected in pp

Table 1: Legendre coefficients obtained from fits to the normalized background-subtracted $\cos \hat{\theta}$ distribution in the four $K^+\pi^-\pi^+$ mass intervals of interest. The up-down asymmetries are obtained from Eq. 4. The quoted uncertainties contain statistical and systematic contributions. The $K^+\pi^-\pi^+$ mass ranges are indicated in GeV/c^2 and all the parameters are expressed in units of 10^{-2} . The covariance matrices are given in the supplementary material.

	[1.1, 1.3]	[1.3, 1.4]	[1.4, 1.6]	[1.6, 1.9]
c_1	6.3 ± 1.7	5.4 ± 2.0	4.3 ± 1.9	-4.6 ± 1.8
c_2	31.6 ± 2.2	27.0 ± 2.6	43.1 ± 2.3	28.0 ± 2.3
c_3	-2.1 ± 2.6	2.0 ± 3.1	-5.2 ± 2.8	-0.6 ± 2.7
c_4	3.0 ± 3.0	6.8 ± 3.6	8.1 ± 3.1	-6.2 ± 3.2
\mathcal{A}_{ud}	6.9 ± 1.7	4.9 ± 2.0	5.6 ± 1.8	-4.5 ± 1.9

Table 2: Legendre coefficients obtained from fits to the normalized background-subtracted $\cos \hat{\theta}$ distribution, using the alternative normal $\vec{p}_{\pi^-} \times \vec{p}_{\pi^+}$ for defining the direction of the photon, in the four $K^+\pi^-\pi^+$ mass intervals of interest. The up-down asymmetries are obtained from Eq. 4. The quoted uncertainties contain statistical and systematic contributions. The $K^+\pi^-\pi^+$ mass ranges are indicated in GeV/c^2 and all the parameters are expressed in units of 10^{-2} . The covariance matrices are given in the supplementary material.

	[1.1, 1.3]	[1.3, 1.4]	[1.4, 1.6]	[1.6, 1.9]
c'_1	-0.9 ± 1.7	7.4 ± 2.0	5.3 ± 1.9	-3.4 ± 1.8
c'_2	31.6 ± 2.2	27.4 ± 2.6	43.6 ± 2.3	27.8 ± 2.3
c'_3	0.8 ± 2.6	0.8 ± 3.1	-4.4 ± 2.8	2.3 ± 2.7
c'_4	3.4 ± 3.0	7.0 ± 3.6	8.0 ± 3.1	-6.6 ± 3.2
\mathcal{A}'_{ud}	-1.1 ± 1.7	7.2 ± 2.0	6.4 ± 1.8	-3.9 ± 1.9

collisions at 7 and 8 TeV center-of-mass energies by the LHCb detector. A total of $13\,876 \pm 153$ signal events is observed. The shape of the angular distribution of the photon with respect to the plane defined by the three final-state hadrons in their rest frame is determined in four intervals of interest in the $K^+\pi^-\pi^+$ mass spectrum. The up-down asymmetry, which is proportional to the photon polarization, is measured for the first time for each of these $K^+\pi^-\pi^+$ mass intervals. The first observation of a parity-violating photon polarization different from zero at the 5.2σ significance level in $b \rightarrow s\gamma$ transitions is reported. The shape of the photon angular distribution in each bin, as well as the values for the up-down asymmetry, may be used, if theoretical predictions become available, to determine for the first time a value for the photon polarization, and thus constrain the effects of physics beyond the SM in the $b \rightarrow s\gamma$ sector.

Acknowledgements

We express our gratitude to our colleagues in the CERN accelerator departments for the excellent performance of the LHC. We thank the technical and administrative staff at the LHCb institutes. We acknowledge support from CERN and from the national agencies: CAPES, CNPq, FAPERJ and FINEP (Brazil); NSFC (China); CNRS/IN2P3 and Region Auvergne (France); BMBF, DFG, HGF and MPG (Germany); SFI (Ireland); INFN (Italy); FOM and NWO (The Netherlands); SCSR (Poland); MEN/IFA (Romania); MinES, Rosatom, RFBR and NRC “Kurchatov Institute” (Russia); MinECo, XuntaGal and GENCAT (Spain); SNSF and SER (Switzerland); NAS Ukraine (Ukraine); STFC (United Kingdom); NSF (USA). We also acknowledge the support received from the ERC under FP7. The Tier1 computing centres are supported by IN2P3 (France), KIT and BMBF (Germany), INFN (Italy), NWO and SURF (The Netherlands), PIC (Spain), GridPP (United Kingdom). We are indebted towards the communities behind the multiple open source software packages we depend on. We are also thankful for the computing resources and the access to software R&D tools provided by Yandex LLC (Russia).

References

- [1] Particle Data Group, J. Beringer *et al.*, *Review of particle physics*, Phys. Rev. **D86** (2012) 010001, and 2013 partial update for the 2014 edition.
- [2] J. C. Pati and A. Salam, *Lepton number as the fourth color*, Phys. Rev. **D10** (1974) 275, Erratum-ibid. **D11** (1975) 703; R. Mohapatra and J. C. Pati, *A natural left-right symmetry*, Phys. Rev. **D11** (1975) 2558; R. N. Mohapatra and J. C. Pati, *Left-right gauge symmetry and an isoconjugate model of CP violation*, Phys. Rev. **D11** (1975) 566; G. Senjanovic and R. N. Mohapatra, *Exact left-right symmetry and spontaneous violation of parity*, Phys. Rev. **D12** (1975) 1502; G. Senjanovic, *Spontaneous breakdown of parity in a class of gauge theories*, Nucl. Phys. **B153** (1979) 334; R. N. Mohapatra and G. Senjanovic, *Neutrino masses and mixings in gauge models with spontaneous parity violation*, Phys. Rev. **D23** (1981) 165; C. Lim and T. Inami, *Lepton flavor nonconservation and the mass generation mechanism for neutrinos*, Prog. Theor. Phys. **67** (1982) 1569; L. L. Everett *et al.*, *Alternative approach to $b \rightarrow s\gamma$ in the $uMSSM$* , JHEP **01** (2002) 022, [arXiv:hep-ph/0112126](#).
- [3] D. Atwood, M. Gronau, and A. Soni, *Mixing-induced CP asymmetries in radiative B decays in and beyond the standard model*, Phys. Rev. Lett. **79** (1997) 185, [arXiv:hep-ph/9704272](#).
- [4] Belle collaboration, S. Nishida *et al.*, *Radiative B meson decays into $K\pi\gamma$ and $K\pi\pi\gamma$ final states*, Phys. Rev. Lett. **89** (2002) 231801, [arXiv:hep-ex/0205025](#).
- [5] BaBar collaboration, B. Aubert *et al.*, *Measurement of branching fractions and mass spectra of $B \rightarrow K\pi\pi\gamma$* , Phys. Rev. Lett. **98** (2007) 211804, [arXiv:hep-ex/0507031](#).

- [6] C. S. Wu *et al.*, *Experimental test of parity conservation in beta decay*, Phys. Rev. **105** (1957) 1413.
- [7] M. Gronau and D. Pirjol, *Photon polarization in radiative B decays*, Phys. Rev. **D66** (2002) 054008, [arXiv:hep-ph/0205065](#).
- [8] E. Kou, A. Le Yaouanc, and A. Tayduganov, *Determining the photon polarization of the $b \rightarrow s\gamma$ using the $B \rightarrow K_1(1270)\gamma \rightarrow (K\pi\pi)\gamma$ decay*, Phys. Rev. **D83** (2011) 094007, [arXiv:1011.6593](#).
- [9] LHCb collaboration, A. A. Alves Jr. *et al.*, *The LHCb detector at the LHC*, JINST **3** (2008) S08005.
- [10] T. Sjöstrand, S. Mrenna, and P. Skands, *PYTHIA 6.4 physics and manual*, JHEP **05** (2006) 026, [arXiv:hep-ph/0603175](#); T. Sjöstrand, S. Mrenna, and P. Skands, *A brief introduction to PYTHIA 8.1*, Comput. Phys. Commun. **178** (2008) 852, [arXiv:0710.3820](#).
- [11] I. Belyaev *et al.*, *Handling of the generation of primary events in GAUSS, the LHCb simulation framework*, Nuclear Science Symposium Conference Record (NSS/MIC) **IEEE** (2010) 1155.
- [12] D. J. Lange, *The EvtGen particle decay simulation package*, Nucl. Instrum. Meth. **A462** (2001) 152.
- [13] P. Golonka and Z. Was, *PHOTOS Monte Carlo: a precision tool for QED corrections in Z and W decays*, Eur. Phys. J. **C45** (2006) 97, [arXiv:hep-ph/0506026](#).
- [14] Geant4 collaboration, J. Allison *et al.*, *Geant4 developments and applications*, IEEE Trans. Nucl. Sci. **53** (2006) 270; Geant4 collaboration, S. Agostinelli *et al.*, *Geant4: a simulation toolkit*, Nucl. Instrum. Meth. **A506** (2003) 250.
- [15] M. Clemencic *et al.*, *The LHCb simulation application, GAUSS: design, evolution and experience*, J. Phys. Conf. Ser. **331** (2011) 032023.
- [16] L. Breiman, J. H. Friedman, R. A. Olshen, and C. J. Stone, *Classification and regression trees*, Wadsworth international group, Belmont, California, USA, 1984.
- [17] R. E. Schapire and Y. Freund, *A decision-theoretic generalization of on-line learning and an application to boosting*, Jour. Comp. and Syst. Sc. **55** (1997) 119.
- [18] T. Skwarnicki, *A study of the radiative cascade transitions between the Upsilon-prime and Upsilon resonances*, PhD thesis, Krakov, PL, Institute of Nuclear Physics, 1986, DESY F31-86-02, Appendix E.
- [19] ARGUS collaboration, H. Albrecht *et al.*, *Search for hadronic $b \rightarrow u$ decays*, Phys. Lett. **B241** (1990) 278.

- [20] M. Pivk and F. R. Le Diberder, *sPlot: a statistical tool to unfold data distributions*, Nucl. Instrum. Meth. **A555** (2005) 356, [arXiv:physics/0402083](#).
- [21] Belle collaboration, H. Yang *et al.*, *Observation of $B^+ \rightarrow K_1(1270)^+\gamma$* , Phys. Rev. Lett. **94** (2005) 111802, [arXiv:hep-ex/0412039](#).

Supplementary material

The covariance matrices obtained from the fit described in the Letter for both photon angle definitions are shown in Tables 3 and 4.

Table 3: Covariance matrices (in units of 10^{-3}) for the fitted values of c_1 , c_2 , c_3 and c_4 of Table 1, for the four $K^+\pi^-\pi^+$ mass intervals.

$$\begin{array}{cc}
 \begin{array}{c} [1.1, 1.3] \text{ GeV}/c^2 \\ \left(\begin{array}{cccc} 0.31 & & & \\ 0.01 & 0.47 & & \\ 0.09 & 0.03 & 0.68 & \\ -0.01 & 0.16 & 0.02 & 0.92 \end{array} \right) \end{array} & \begin{array}{c} [1.3, 1.4] \text{ GeV}/c^2 \\ \left(\begin{array}{cccc} 0.41 & & & \\ 0.02 & 0.66 & & \\ 0.12 & 0.04 & 0.93 & \\ 0.00 & 0.20 & 0.04 & 1.27 \end{array} \right) \end{array} \\
 \begin{array}{c} [1.4, 1.6] \text{ GeV}/c^2 \\ \left(\begin{array}{cccc} 0.35 & & & \\ -0.01 & 0.52 & & \\ 0.14 & 0.00 & 0.76 & \\ -0.03 & 0.23 & -0.01 & 0.99 \end{array} \right) \end{array} & \begin{array}{c} [1.6, 1.9] \text{ GeV}/c^2 \\ \left(\begin{array}{cccc} 0.34 & & & \\ -0.02 & 0.51 & & \\ 0.08 & -0.04 & 0.75 & \\ -0.02 & 0.15 & -0.04 & 1.01 \end{array} \right) \end{array}
 \end{array}$$

Table 4: Covariance matrices (in units of 10^{-3}) for the fitted values of c'_1 , c'_2 , c'_3 and c'_4 of Table 2, for the four $K^+\pi^-\pi^+$ mass intervals.

$$\begin{array}{cc}
 \begin{array}{c} [1.1, 1.3] \text{ GeV}/c^2 \\ \left(\begin{array}{cccc} 0.30 & & & \\ 0.00 & 0.47 & & \\ 0.09 & 0.02 & 0.68 & \\ 0.02 & 0.16 & 0.02 & 0.92 \end{array} \right) \end{array} & \begin{array}{c} [1.3, 1.4] \text{ GeV}/c^2 \\ \left(\begin{array}{cccc} 0.41 & & & \\ 0.03 & 0.66 & & \\ 0.12 & 0.07 & 0.93 & \\ 0.01 & 0.20 & 0.10 & 1.27 \end{array} \right) \end{array} \\
 \begin{array}{c} [1.4, 1.6] \text{ GeV}/c^2 \\ \left(\begin{array}{cccc} 0.35 & & & \\ 0.01 & 0.53 & & \\ 0.14 & 0.05 & 0.76 & \\ 0.00 & 0.24 & 0.03 & 0.99 \end{array} \right) \end{array} & \begin{array}{c} [1.6, 1.9] \text{ GeV}/c^2 \\ \left(\begin{array}{cccc} 0.34 & & & \\ 0.00 & 0.51 & & \\ 0.08 & 0.00 & 0.75 & \\ 0.02 & 0.15 & -0.01 & 1.01 \end{array} \right) \end{array}
 \end{array}$$